Ecological Modelling 382 (2018) 18–32

Contents lists available at ScienceDirect

Ecological Modelling

journal homepage: www.elsevier.com/locate/ecolmodel

# A physiologically inspired agent-based approach to model upstream passage of invasive fish at a lock-and-dam

D.P. Zielinski[a,b,*,1], VR. Voller[c], P.W. Sorensen[a]

[a] Department of Fisheries, Wildlife, and Conservation Biology, University of Minnesota, St. Paul, MN, USA
[b] Great Lakes Fishery Commission, Ann Arbor, MI, USA
[c] Department of Civil, Environmental, and Geo- Engineering University of Minnesota, St. Paul, MN, USA

ARTICLE INFO

*Keywords:*
Computational fluid dynamics
Fish passage
Asian carp
Agent-Based
Lock-and-dam
Mississippi River

ABSTRACT

The ability of fish to swim upstream through regions of swiftly flowing water is ultimately dependent on their physiological capacity. Swimming performance, the relationship between swim speed and time-to-fatigue, has been used to design fishways and identify barriers to fish movement. However, existing numerical models do not all capture the variability in swimming abilities nor the turbulent, unsteady, and three-dimensional aspect of natural flows. This deficiency is particularly problematic for fish species whose behavior is poorly understood (i.e., invasive fish) and at sites with complex flow patterns. Here, we combine species-specific swimming performance with high resolution abstractions of fluid flow in a new agent-based framework to model fatigue of upstream swimming fish under turbulent flow conditions. Our model simulates fish paths, in the absence of information on their behavioral tendencies, based on a rules-set aimed at fish swimming as far upstream as possible before complete exhaustion by selecting the path of least fatigue. We demonstrate how this model functions by examining theoretical passage of invasive silver carp, Hypopthalmichthys molitrix, and bighead carp, H. nobilis, as well a native fish, the lake sturgeon, Acipenser fulvescens, through a typical Mississippi River lock-and-dam (Lock-and-Dam #8 near Genoa, WI). The model then tests whether passage could be reduced by altering spillway gate operations. Model results suggest that passage of all three species is low under current gate operations and that passage of both carp species could be further reduced by about half through minor changes in spillway gate operation without apparent impacts on navigation, scour, or lake sturgeon passage. Model results are qualitatively consistent with observed passage rates monitored by other studies at similar lock-and-dams and are consistent with the possibility that the model likely overestimates passage rates by relying on physiological data only. This approach could be exported to other applications and fish species to help manage and control fish migration and dispersal, especially for fish whose behavior and ecology are poorly understood and not presently quantifiable.

## 1. Introduction

Fish migration and dispersal are key life history traits that are highly susceptible to disruption by natural and man-made obstructions like waterfalls, dams, and culverts. Upstream movement in particular is heavily impacted by hydraulic challenges (i.e., regions of flow that exceed a fish's locomotor capacity). However, while understanding how fish movement is influenced by water flow is vital to the design of fishways and identification of barriers to movement, relating fish movement to the naturally unsteady, turbulent, and three-dimensional flow conditions found in these situations is not straightforward (Liao et al., 2003). Accordingly, fisheries managers and engineers have developed computer models to help bridge the gap between water flow and fish movement. Preferably, models of fish movement would incorporate environmental stimuli (e.g., velocity, temperature, etc.) with data on physiology (e.g., swimming performance) and key information on behavioral attributes (e.g., when and why particular fish move). However, while both environmental stimuli and physiological traits of certain species of fish are often either well understood or readily obtained using laboratory instrumentation (e.g., swim tunnels); fish behavior, especially in situ, is inherently difficult to obtain and usually unavailable. Thus, with the exception of a handful of economically important species (e.g., Pacific salmon, freshwater eels), behavioral traits of upstream swimming fish in the field are largely unknown. This

* Corresponding author at: Great Lakes Fishery Commission, Ann Arbor, MI, USA.
*E-mail address:* dzielinski@usgs.gov (D.P. Zielinski).
[1] Current address: Great Lakes Fishery Commission, 11188 Ray Road, Millersburg, Michigan, 49759-9481, USA.

https://doi.org/10.1016/j.ecolmodel.2018.05.004
Received 3 January 2018; Received in revised form 4 May 2018; Accepted 4 May 2018
Available online 10 May 2018
0304-3800/ Published by Elsevier B.V.

is especially the case for non-native fishes, some of which are invasive. Since many existing models require information on behavioral traits, which is lacking for invasive species, new models that emphasize physiological limits of fish swimming (i.e., how fast and how long can fish swim before exhaustion) to examine barriers to fish passage and estimate movement ranges are needed.

One area where modelling of the physiological limits of fish movement in complex flows would be especially beneficial is the control of invasive species such as the Asian or bigheaded carps (a genus with two key species, the silver carp, Hypopthalmichthys molitrix and bighead carp, H. nobilis). The bigheaded carps are large, voracious microphagous fish that were introduced to North America in the 1970s (Kolar et al., 2007) and are now disrupting food webs and negatively impacting fisheries across the Mississippi River Basin (Carlson et al., 1995; Schrank et al., 2003; Sass et al., 2014; Pendleton et al., 2017). However, while they are ubiquitous in much of this large watershed, they have not yet invaded many peripheral and interconnected areas including the Mississippi River headwaters area, upper Illinois River, and the Great Lakes (USFWS, 2014). Identifying new ways to block upstream movement of bigheaded carp is a key objective of state, regional, and federal management strategies in these regions (Tsehaye et al., 2013). The set of 29 Mississippi River navigational lock-and-dams located in this river network and managed by the U.S. Army Corps of Engineers (USACE) offers a possible avenue to block bigheaded carp passage as all fish must pass through them. Water velocities increase as a result of passing through the lock-and-dam spillway gates which are also fully adjustable and have already been suggested to reduce passage of native migratory species in the Mississippi River (Knights et al., 2002; Zigler et al., 2003, 2004). Further, a recent swim study on bigheaded carp swimming performance (Hoover et al., 2017) showed that bigheaded carps are relatively weak swimmers. The possibility that lock-and-dams could be used to block passage has also been supported by telemetry studies at lock-and-dams in the Mississippi River (Tripp et al., 2014) and Illinois River (Lubejko et al., 2017), which found bigheaded carp passage rates to be low and occur largely during open-river conditions (i.e., all spillway gates are raised out of the water and velocities are relatively low). Lock-and-dams near the headwaters of the Mississippi River, where bigheaded carp have not yet reached, rarely experience open-river conditions (FishPro, 2004) and represent the greatest likely impediment to fish passage (depending on when specific fishes naturally move relative to open-river conditions). If gate operations could be modified in appropriate ways that do not increase scour near the structure or impair navigation, these lock-and-dams would offer great potential to further restrict bigheaded carp passage. However, flows through these structures are complex and not easily measured, and there are presently no data on carp behavior or movement near these structures. Models must therefore rely on swimming performance and hydraulic data alone. A common approach to such models is to assume fish will swim to their maximum physiological capacity (e.g., exhaustion), resulting in conservative estimates of passage as fish are not naturally expected to swim to complete exhaustion. Models that calculate the highest number of fish passing a hydraulic challenge are of great value as a first step to evaluate whether and how to stop undesirable invasive species while allowing for the possible passage of other species like the lake sturgeon, Acipenser fulvescens, a native fish of ecological and cultural importance that makes prolonged migrations throughout the Mississippi River Basin.

In this study we develop a new numeric model to describe fish swimming upstream through a hydraulic challenge by incorporating species-specific data on fish swimming performance and hydraulic data around and through structures such as locks-and-dams. We then use the model to both evaluate, and then simulate, fish passage through a typical lock-and-dam under various scenarios while comparing findings with known data at similar structures. It is novel because of the manner in which we merge two attributes, swimming performance and hydraulic conditions, the first of which we now introduce. Fish swimming performance (i.e., the relationship between swim speed and time-to-fatigue) is generally categorized by two distinct modes: sustainable and unsustainable swimming. While fish can maintain relatively slow swim speeds almost indefinitely by relying on aerobic metabolism (i.e., sustainable swimming), they cannot do this at higher speeds as their ability to swim become limited by the contribution of anaerobic metabolism (i.e., unsustainable swimming). Further, fish can only maintain unsustainable swim speeds for limited durations that are inversely related to swim speed (Beamish, 1978). Thus, after bouts of unsustainable swimming, fish completely fatigue, and may require several hours to recover (see review in Kieffer (2000)). Relationships between swim speed and time-to-fatigue are readily quantified through laboratory swim tunnel / flume trials (Beamish, 1978; Castro-Santos, 2005; Hoover et al., 2017).

Hydraulic conditions are the second key component of our model. They can be generated using well-established computational fluid dynamics (CFD), computer models that simulate water flows by solving the governing equations of fluid flow, and is a practical method to model the complex flows in and around lock-and-dams in a framework that fish passage can be readily incorporated. Since CFD models provide fine-scale resolution (i.e., sub-meter, seconds/minutes) hydraulic data over a wide range of conditions, it is already widely incorporated into modelling applications focused on the interface of hydraulics and ecology (Daraio et al., 2010; Harvey and Clifford, 2009). Generating fine-scale simulations of flow fields experienced by fish is critical as the efficacy of any model or assessment of fish movement is inexorably linked to the scale at which spatiotemporal changes in water velocity are modeled (Tullos et al., 2016). Our approach is driven by the need to expand upon existing fish passage models which either are limited by reliance upon simplified hydraulics and homogenized swimming performance (ex. FishXing; Furniss et al., 2006) or require extensive (usually nonexistent) telemetry data (Gao et al., 2016; Arenas et al., 2015; Goodwin et al., 2014, 2006; Haefner and Bowen, 2002) Also, with the exception of Gao et al. (2016), all extant behavioral models are intended to describe downstream movement of fish where the influence of swimming fatigue is minimized.

In this study, we develop and describe a new agent-based approach, a mathematical model that simulates the interactions of individuals, or agents, with each other and/or their environment. Our model incorporates swimming performance data with high resolution abstractions of complex fluid environments to evaluate fish swimming fatigue. Agent-based approaches similar to this have proven to be effective in simulating many complex ecological phenomena like larval fish navigation (Staaterman and Paris, 2004), fish aggregations and movement (Gao et al., 2016; Arenas et al., 2015; Goodwin et al., 2014, 2006; Nestler et al., 2002; Huth and Wissel, 1992), and mussel dispersal (Daraio et al., 2010), but they have not been deployed to understand invasive fish passage at lock-and-dams before. Our model makes three primary assumptions: (1) fish are only motivated to move upstream (i.e., no backtracking); (2) fish swim at their distance-maximizing ground speed; and (3) fish select a path of least energetic cost. The percent endurance model, developed by Castro-Santos (2005) and partially used in other fish passage evaluations (Neary, 2012) is used as a proxy for energy expenditure. Stochasticity is introduced by varying individual fish swimming performance and hydraulic fields based on turbulent fluctuations.

We describe the framework of a new agent-based swimming fatigue model and discuss its general characteristics and intrinsic models. We then demonstrate the applicability of the model by simulating bigheaded carp passage at Lock-and-Dam #8 (Genoa, WI) on the Mississippi River, a structure with similar geometry and hydrologic features to many other lock-and-dams and located upstream of the bigheaded carp invasion front. We examine whether these invasive species are likely being blocked by current spillway gate operations at this typical lock-and-dam and whether changes to gate operating procedures (i.e., gate opening height) could enhance this feature without

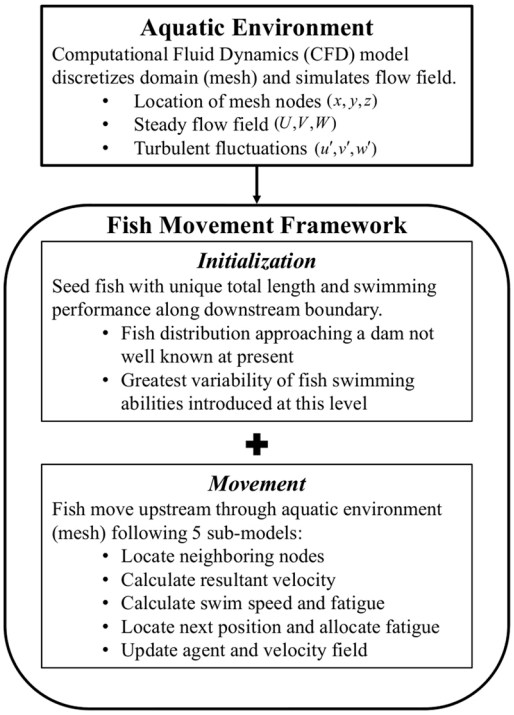


**Fig. 1.** Schematic representation of the agent-based fish fatigue model to simulate swimming pathways through complex flows that require the least energy. The model primarily consists of an aquatic environment (i.e., flow field) and fish component. Fish movement is based on individual size and swimming performance metrics following a rules set made of 5 sub-models. Descriptions of the sub-models are provided in Section 2.2.

impacting navigation, scour or passage of lake sturgeon. We qualitatively compare model results to observed fish passage rates at other Mississippi River lock-and-dams. We also evaluate whether and how different gate operating procedures might alter the use of the navigational locks and scour downstream of the lock-and-dam.

## 2. Methods

We develop a new type of agent-based model to evaluate upstream swimming capabilities of fish based on swimming performance and then explore how it can be applied. This fish swimming fatigue model is comprised of an environmental domain (i.e., flow field) in which agents (i.e., fish) are inserted and move throughout (Fig. 1). The aquatic environment is represented by a computational mesh (i.e., spatial grid of elements) (Fig. 2) where the location of each element, water depth, and water velocity are simulated using hydraulic models. Individual fish follow predefined movement rules in response to local hydraulic conditions (e.g., velocity vectors). When we force simulated fish to seek routes requiring the least amount of energy (McElroy et al., 2012), the model can reveal which pathways fish must take to cover the maximum upstream distance possible. These pathways emerge from the interaction of local hydraulic conditions and theoretical swimming performance. Once identified, we investigate how passage along these paths can be increased (or decreased) by modifying the hydraulic conditions at our model site. Although there are many possible pathways fish can take through a complex flow environment, we focus on the path with the least energetic cost as all other paths would be higher energy paths and less likely to lead to successful passage – and we are interested in determining the highest possible number of fish passing the lock-and-dam. Following the schematic representation of the model in Fig. 1, we first describe how the aquatic environment and fish movement are represented, and conclude with a demonstration of the model to identify how invasive bigheaded carps may already be moving through a typical Mississippi River lock-and-dam and then how gate operations at this structure could be altered to block bigheaded carp.

### 2.1. Aquatic environment

We determine 3D simulations of the flow field using the ANSYS (Release 17.1) Fluent CFD software package. The Reynolds-averaged Navier-Stokes (RANS) equations and k-ε turbulence model with wall functions are solved using the finite volume method. Pressure and velocity are coupled using the Semi-Implicit Method for Pressure Linked Equations (SIMPLE) algorithm, and second-order discretization schemes are used for the convection and viscous terms of the governing equations. Unstructured tetrahedral meshes (i.e., spatial grid of elements within which discrete versions of the governing equations are solved) are generated using the ANSYS Workbench meshing application (Fig. 2). Unsteady RANS modeling is required to appropriately model complex flow at high Reynolds numbers (Spalart, 2000) and to obtain the mean velocity (U, V, W) and distribution of turbulent fluctuations ($u'$, $v'$, $w'$) at all nodes in the fluid domain. The instantaneous velocity at all nodes is described by:

$$\begin{aligned} u(x, y, z) &= U(x, y, z) + u'(x, y, z) \\ v(x, y, z) &= V(x, y, z) + v'(x, y, z) \\ w(x, y, z) &= W(x, y, z) + w'(x, y, z) \end{aligned} \quad (1)$$

where u, v, and w are the instantaneous velocity in the x-, y- and z-direction. CFD models are run using a cluster node equipped with two 2.4 Ghz 14-core Intel Xeon processors and 128 GB memory.

### 2.2. Fish movement framework

We examine fish movement through the field using an agent-based approach to model fish movement and fatigue. This process begins with an initialization step followed by a movement step, which has several sub-models.

#### 2.2.1. Initialization

We start by generating numeric fish (agents) with unique swimming performance metrics and total length. Swimming performance metrics for each individual fish are selected randomly from swim speed-fatigue time curves (see Section 2.2.2.3) normalized by total body length based on experimental data (mean estimates of coefficients a and b with standard deviation $\sigma_a$ and $\sigma_b$, and sustained swim speed limit). Once coefficients are selected, swim speed-fatigue relationships are transformed by total body length to create fish with unique swimming abilities. This approach is similar to methods outlined by Castro-Santos (2006), combining unique individual total lengths and normalized swimming performance metrics simulates natural biological variation and yield individuals with a range of swimming abilities (e.g., small-fast fish vs. large-slow fish). Fish are then randomly seeded along the downstream boundary of the flow field following a uniform distribution. A uniform distribution is used in lieu of observed approach patterns and to ensure simulated fish approach a hydraulic challenge from as many different trajectories as possible.

#### 2.2.2. Movement

Once seeded, each fish advances upstream through the flow field by marching through nodes from the computational mesh following a step selection process that follows the upstream pathway that causes the least fatigue without backtracking and swimming at a theoretical distance maximizing ground speed (see Section 2.2.2.3) (Castro-Santos, 2005). At each node, fish "survey" neighboring nodes upstream of their current location for fatigue that would result from swimming to each node using the resultant velocity acting between the initial node and each neighboring node (Fig. 3). The fish then selects and moves to the node that results in the lowest possible fatigue. Each simulation repeats

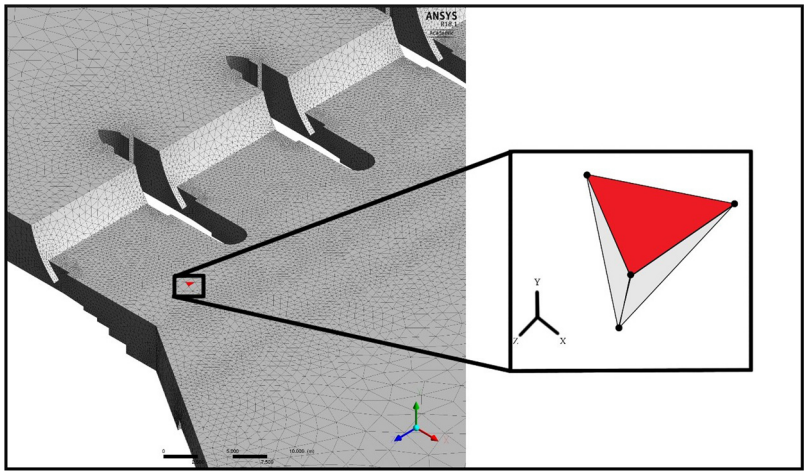

**Fig. 2.** Example of computational mesh generation showing an unstructured 3D tetrahedral mesh with inset of an individual element in the mesh with nodes (black dots) located at the corners of the element. Field data are stored at the nodes.

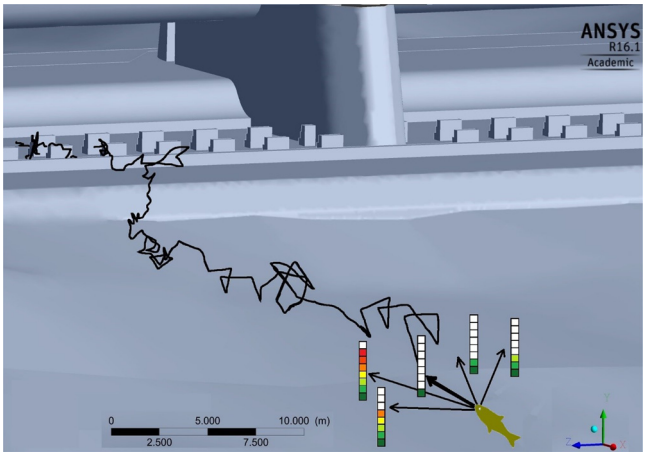


**Fig. 3.** Illustrated schematic of agent-based fish swimming fatigue model. Fish sample the incremental fatigue caused to swim to each of the neighboring nodes. Vertical bars indicate relative fatigue related to swimming to each neighboring node. The example shows a fish selecting the lowest fatigue path at a local level (arrows indicate potential paths) and domain level (solid black line indicates pathway followed).

this process for every fish until they completely exhaust or reach the upstream boundary of the flow field.

The process occurs via 5 sub-models that follow the process outlined in Fig. 1. The sub-models address: (1) finding the upstream nodes neighboring the fish's current location; (2) calculating the resultant velocity fish must swim against; (3) calculating the swim speed and fatigue; (4) locating the next position and allocating fatigue; and (5) updating the agent variables and velocity field.

*2.2.2.1. Sub-model 1: Locate neighboring nodes.* In this sub-model, fish search through the computational mesh to locate potential locations to move that are positioned in front of its current location and are within a specified sensory range, δ (see Fig. 4). Since fish are assumed to be motivated to only move upstream, only nodes located within an 180° arc upstream of the fish's position were considered (i.e., no backtracking). To ensure fish do not bypass regions of higher velocity that cannot otherwise be avoided, δ was set to half the total length of the fish (i.e. approximately three times the minimum node spacing for the smallest modeled fish). If less than 3 nodes were located within this hemisphere, δ was doubled until 3 or more nodes were present. This limit was set to force fish to survey across a minimum number of movement directions and prevent fish movement paths from being overly restricted by node locations. Without this requirement, fish could be forced to move to a node because of its proximity and not local hydraulic conditions. As a measure to reduce computation time, δ was set to twice the total body length in areas where the mesh is coarse (nodes spaced 1–1.5 m apart) and velocity gradients are low.

*2.2.2.2. Sub-model 2: Calculate resultant velocity.* A resultant velocity is calculated for each neighboring node determined in the previous section. We used resultant velocity instead of velocity magnitude as it enables modifications which allow for the direction of fluid flow to either aid or hinder movement. If the flow vector at the neighboring node acts in the same direction as the potential swim vector, the velocity fish must overcome is reduced (i.e., fish movement is potentially aided by flow direction). For any initial point ($x_o$, $y_o$, $z_o$) and neighboring node ($x_i$, $y_i$, $z_i$) with velocity vector ($U_i$, $V_i$, $W_i$) and depth below the water surface $d_i$, the resultant velocity can be written as

$$U_{res} = \sqrt{(U_N^2 + V_N^2 + W_N^2)} \tag{2}$$

where $U_N$, $V_N$, $W_N$ are conditional velocity components dependent on the direction of movement between the initial point and neighboring node and velocity vector (Fig. 4). The conditional velocity component in the horizontal plane is defined as

$$U_N = \begin{cases} U_i, & \frac{\Delta x}{|\Delta x|} \neq \frac{U_i}{|U_i|} \\ 0, & \frac{\Delta x}{|\Delta x|} = \frac{U_i}{|U_i|} \end{cases} \tag{3}$$

in the x-direction, and

$$V_N = \begin{cases} V_i, & \frac{\Delta y}{|\Delta y|} \neq \frac{V_i}{|V_i|} \\ 0, & \frac{\Delta y}{|\Delta y|} = \frac{V_i}{|V_i|} \end{cases} \tag{4}$$

in the y-direction when the direction of movement is defined as

$$\Delta x = x_i - x_o$$
$$\Delta y = y_i - y_o \tag{5}$$

Using this arrangement, if the horizontal direction of movement between the initial position and next node are oriented in the same direction as the velocity component, that portion of the velocity vector is set to zero in Eqs. (3) and (4). For example, if the fish was to move to node 7 in Fig. 4A, the horizontal velocity component, $U_N$, would be set to zero because is acts in the same direction as the fish movement.

Movement in the vertical plane is dependent on both the velocity direction and position relative to the preferred depth of the fish

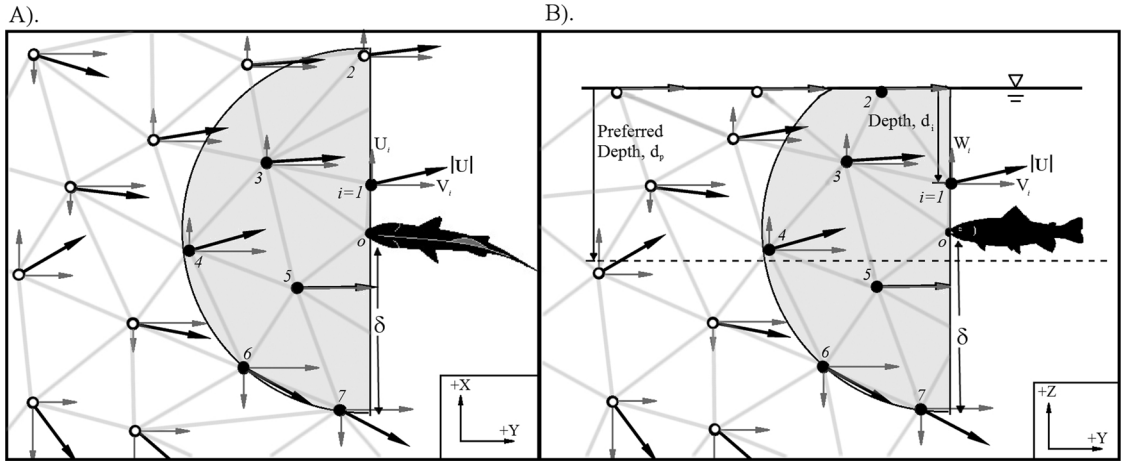


**Fig. 4.** Calculation of resultant velocity acting on fish in the (A) horizontal and (B) vertical planes. Circles indicate mesh nodes, dark arrows are velocity magnitude, grey arrows are velocity components, and shaded area encloses the nodes being evaluated within a distance, δ, from the fish. The resultant velocity is the magnitude of the velocity vector acting between the initial node and each neighboring node in opposition to the direction of movement. Light gray lines denote the computational mesh.

(Fig. 4B). Fish regulate depth by altering the volume of their swim bladder. Since this process takes several minutes to achieve even a slight change in density (i.e. time to change swim bladder volume > time to pass hydraulic challenge) (Strand et al., 2005), fish are assumed to attempt passage with a constant swim bladder volume and thus a preferred depth, $d_p$. The conditional velocity component in the vertical direction is then defined as:

$$W_N = \begin{cases} W_i, & d_i < d_p \cup W_i > 0 \\ 0, & d_i < d_p \cup W_i < 0 \\ W_i, & d_i > d_p \cup W_i < 0 \\ 0, & d_i > d_p \cup W_i > 0 \end{cases} \quad (6)$$

In this arrangement, the vertical velocity component contributes to the resultant velocity only when the vertical velocity acts against the fish trying to return to its preferred depth.

*2.2.2.3. Sub-model 3: Calculate swim speed and fatigue.* We estimated the swim speed and time-to-fatigue for each individual fish based on swimming performance data collected from swim tunnel tests. When swim speeds exceed a fish's maximum sustained swim speed, $U_{sus}$,the relationship between swim speed, $U_s$, and endurance (i.e., time-to-fatigue), T, generally follows a log-linear model (Castro-Santos, 2005; Peake et al., 1997)

$$\ln T = a + bU_s, \; b < 0 \quad (7)$$

where $a$ and $b$ are the slope and intercept coefficients fit from experimental data. Swim speed can then be related to ground speed, $U_g$, by

$$U_g = U_s - U_{res} \quad (8)$$

where $U_{res}$ is the resultant water velocity assumed to act against fish movement. The distance swam can then be found as the product of ground speed and endurance. Castro-Santos (2005) used this relationship to derive a theoretical distance maximizing ground speed as:

$$U_{gOPT} = -1/b \quad (9)$$

The concept of distance maximizing ground speed is important because it assumes fish constantly adjust their swimming speed with water velocity to swim the maximum possible distance.

If $U_{res} < U_{sus}$, fish were assumed to swim at a speed equal to $U_{sus}$ and incur no fatigue. However, when $U_{res} \geq U_{sus}$ fish must swim at unsustainable speeds (i.e., requiring some level of anaerobic fueling) to continue upstream. To ensure fish reach as far upstream as possible through the flow field while swimming at unsustainable speeds, the ground speed was assumed to be equal to the distance maximizing ground speed (Castro-Santos, 2005) according to in Eq. (9). The time, Δt, for fish to swim between neighboring nodes can then be calculated as

$$\Delta t = l/U_{gOPT} \quad (10)$$

where l is the distance between nodes.

Calculation of fatigue caused by fish swimming from their initial position to each of the neighboring nodes follows the percent-endurance model (Castro-Santos, 2006; Neary, 2012). Given the fish's endurance, T, for a given effort and time required to swim between nodes, Δt, the percent fatigue, ΔF, expended by fish to reach the next node can be derived as

$$\Delta F = \begin{cases} \frac{\Delta t}{T} \times 100\%, & U_{res} \geq U_{sus} \\ 0, & U_{res} < U_{sus} \end{cases} \quad (11)$$

The fish's endurance, T, is not static, but is recalculated during each step based on the required swim speed to reach the neighboring node. This approach assumes fish have a predetermined energy budget and discrete bouts of swimming between nodes incrementally decreases the budget, which, if used entirely, leads to complete exhaustion and termination of the passage attempt.

Unsustainable swimming is commonly divided into two distinct modes: prolonged and burst (Castro-Santos, 2005). Prolonged mode swimming is fueled by a mixture of anaerobic and aerobic metabolism that can be maintained for 20 s – 200 min, while burst mode swimming is fueled entirely by anaerobic metabolism and can typically only be maintained for < 20 s (Beamish, 1978). For each mode, the relationship between swimming speed and endurance still follows Eq. (7), but with unique coefficients (Castro-Santos, 2006). Notably, the distance maximizing ground speed (Eq. (9)) would also be unique for each swimming mode. The percent-endurance model can be modified to estimate fatigue during both prolonged and burst swim modes (Castro-Santos, 2006; Neary, 2012).

*2.2.2.4. Sub-model 4: Locate the next position and allocating fatigue.* Step selection assumes fish follow the upstream pathway that causes the least amount of fatigue without backtracking. At each decision point, all neighboring nodes are surveyed based on percent fatigue. In the event all neighboring nodes cause fatigue, the node with the minimum percent fatigue is chosen. In all other situations, where at least one

node does not cause fatigue, the new position of the fish is selected at random from the group of non-fatigue causing nodes. Because only nodes in front of the fish are surveyed, the effect of the random node selection makes the default movement pattern reflect a biased random walk. Once the new position is selected, the total fatigue, F, is updated based on the percent fatigue incurred during movement. This way, the total fatigue at any point along a given pathway is the accumulation of $\Delta F$ at all prior steps. Complete exhaustion occurs when $F = \Delta F_j + \Delta F_{j=1} + \cdots + \Delta F_n \geq 100\%$, where $j = 1,2, \cdots, n$ denotes each step.

*2.2.2.5. Sub-model 5: Update agent and velocity field.* After each step selection the velocity field is updated (i.e., turbulent fluctuations approximated) and agent variables are recorded. The velocity field is updated by augmenting the steady state velocity with an approximation of turbulent fluctuations by selecting a new water velocity at each node from a normal distribution with mean (U, V, W) and standard deviation ($u'$, $v'$, $w'$). This step incorporates turbulence into the flow field using a stochastic approach rather than attempting to directly correlate fish movement with specific time steps of an unsteady flow condition. The agent variables recorded after each step include: fish location (x, y, z), water depth (d), distance traveled (l), resultant velocity ($U_{res}$), swimming speed ($U_{sus}$), percent fatigue ($\Delta F$), and swimming time ($\Delta t$). A collective summary of fish total length (TL), starting coordinates, and binary passage result (0 = success, 1 = failure) is also recorded. Passage success is quantified by fish reaching a predetermined distance past a hydraulic challenge.

### 2.3. Applying the model to a typical Mississippi River lock-and-dam to evaluate fish passage

To demonstrate the functionality of our agent-based model, it was applied at Lock-and-Dam #8 (Genoa, WI) (Fig. 5A) to determine first how current gate operations might be blocking bigheaded carp passage, and then how this attribute might be enhanced. Lock-and-Dam #8 has similar operation and geometry to other lock-and-dams in the Upper Mississippi River. Flow through Lock-and-Dam #8 is controlled by two types of spillways gates: 1) ten 10.7 m wide tainter gates and 2) five 24.4 m wide roller gates. The adjacent lock chamber is 152.4 m long x 33.5 m wide (Fig. 5B). To pass flow, both sets of spillway gates raise off the river bottom following a pre-determined operating schedule as documented in the USACE Water Control Manual (USACE, 2003). Water velocity through the gated openings is generally the greatest when the gates are barely open and decreases as the gates are raised. When the gates are raised completely out of the water, the dam is in so-called "open-river" conditions. Existing gate operating procedures aim to produce a uniform velocity distribution which does not exceed a depth averaged velocity of 1.5 m/s at the endsill of the structure which is situated ~23 m downstream of the roller gates and ~17 m downstream of the tainter gates (USACE, 2003). Discharge rating curves for each gate type were established by the USACE using velocity data collected from Acoustic Doppler Current Profiler (ADCP) surveys ~100 m downstream and a physical model study (Markussen and Wilhelms, 1987) but has never been modeled using CFD. Existing gate operation procedures dictate all tainter gates are opened to one uniform height and all roller gates are opened to a different uniform height. The lock was not considered in our model because they have minimal attraction flow for fish, operate intermittently with boat traffic, and are not considered sustainable pathways for fish passage (Wilcox et al., 2004).

#### 2.3.1. CFD models

3D CFD simulations were first run for five river discharges: 625, 1250, 1475, 2325, and 2720 $m^3/s$ at Lock-and-Dam #8 (see Table 2 for gate positions). These flows represent the full range of gate controlled flows (i.e. open-river conditions at 2720 $m^3/s$). CFD velocity fields were qualitatively validated using ADCP surveys ~100 m downstream and results from a physical model study (Markussen and Wilhelms, 1987) (see Supplemental Figs. 1–12). Additional CFD models of river discharge 1755 and 2067 $m^3/s$ were performed and qualitatively validated with physical model studies to further ensure CFD model accuracy, but not analyzed for fish passage. Unstructured tetrahedral meshes ($> 10^6$ nodes) were generated using the ANSYS Workbench meshing application. The mesh sizes ranged from 0.15 to 1.5 m (~1-2 million nodes). Construction drawings and sub meter resolution river soundings data provided by the USACE were used to generate boundaries for the CFD modelling. Upstream boundary conditions were specified as a uniform depth averaged velocity. The downstream boundary was set as an outflow boundary where the diffusion flux of all variables was set to zero. No-slip (zero-fluid-velocity) boundaries were set at all solid surface interfaces and surface roughness (roughness height of 0.03 m for all concrete surfaces and 0.3 m for river substrate) was accounted for by applying the modified law-of-the-wall equations and velocity shift formulas. Water surface boundary conditions were treated as a rigid lid (i.e., zero shear stress) set to match the longitudinal water surface profile obtained from gauge records. Although a rigid lid assumption can induce errors in velocity field calculations in areas were the water

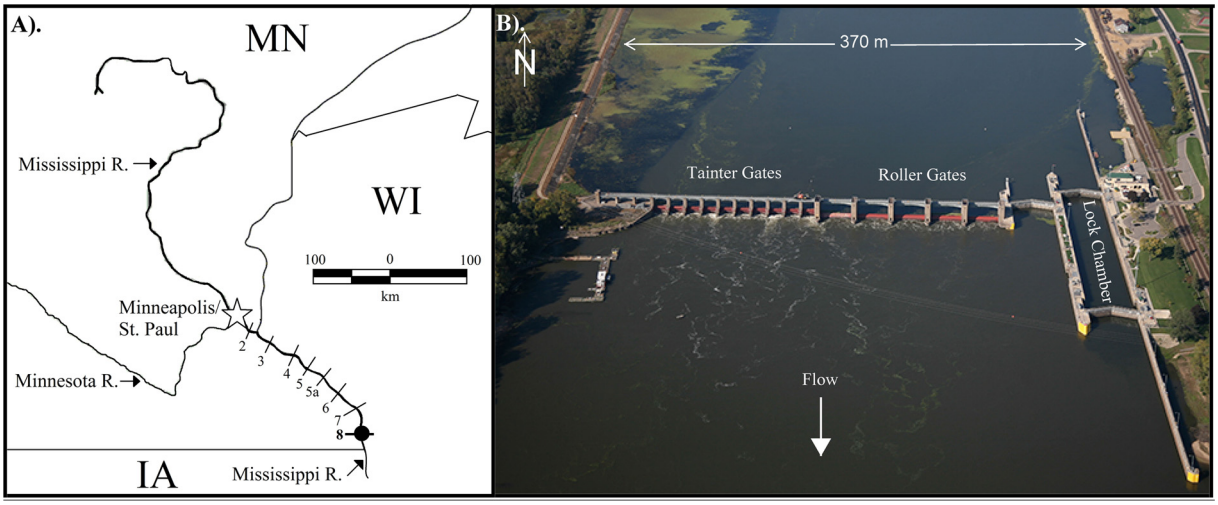


**Fig. 5.** (A) Map showing the locations of navigational lock-and-dams (represented as bars and labeled by number) on the Mississippi River. (B) Aerial photograph of Lock-and-Dam #8 (43°34′12″N 91°13′54″W). Photo taken by U.S. Army Corps of Engineers (USACE). Flows are controlled at Lock-and-Dam #8 by ten 10.7 m wide tainter gates and five 24.4 m wide roller gates. The lock chamber is 152.4 m long × 33.5 m wide.

surface fluctuates substantially, the water surface downstream of Mississippi River lock-and-dam spillways experience only minor fluctuations due to the bottom release of water. The rigid lid assumption was considered reasonable due good agreement with the physical model study that collected profiles of velocities through the spillway. Symmetry boundary conditions were set along portions of the right river bank (looking downstream) where river soundings were not available. A hybrid initialization process was used to set the velocity field and domain averaged values for turbulence variables within the fluid domain. The unsteady solution, used to generated turbulent statistics used in Eq. (1), was run to a quasi-steady state (solution converges in a statistical sense) with convergence criteria for residuals set at $10^{-4}$. Unsteady calculations were run with a time step of $\Delta t = 0.2$ s with a maximum of 15 dual-time-stepping iterations per physical time step. A first-order implicit solver was used to simulate 1000 physical time steps. Following Ge and Sotiropoulos (2005), the unsteady solution was considered converged once the difference between instantaneous velocity fluctuations about the mean were an order of magnitude less than the mean.

Post-processing of the CFD data (e.g. velocity data and mesh coordinates) included modifying the domain with artificial boundaries to create convex surfaces to prevent fish from getting "stuck" (i.e., accessing regions where no continuous upstream pathways are available). Because the model prevents fish from backtracking, in an unmodified domain, instances could occur where fish move behind a spillway gate or lock chamber and are unable to pass without backtracking. To remedy this situation, artificial boundaries were constructed downstream of each tainter gate (i.e. the gate's curve creates a region where fish can get stuck) and the lock chamber. At the tainter gates, an artificial boundary was applied along a plane extending downstream from the lip of the gate and back to the water surface along a 1:1 slope. At the lock chamber an artificial boundary was applied along a plane extending downstream from the apex of the interior lock wall across the lock chamber at a 1:1 slope. These boundaries did not change the velocity field, but merely prevent fish from accessing these regions and direct fish upstream.

#### 2.3.2. Modeling fish passage under current USACE gate operating procedures

Our fish passage model was used to simulate movement of silver carp, bighead carp, and a native species with known swimming performance, the lake sturgeon, through Lock-and-Dam #8. For each species, 5000 fish (agents) were assigned a total body length from one of five 100 mm size classes adapted from published population size distributions. These were adapted from Seibert et al. (2015) for silver carp (TL 600–1000 mm), Schrank and Guy (2002) for bighead carp (TL 700–1100 mm), and Mcdougall et al. (2013) for lake sturgeon (TL 900–1300 mm) in other large rivers as no data existed for Lock-and-Dam #8 (See Supplementary Fig. 13). These locations were believed to have relatively large (unexploited) fish, thus making our models "conservative" or likely to overestimate passage. Because silver and bighead carps are pelagic feeders, they were assigned a preferred depth of 1 m; whereas lake sturgeon, a benthic species, was assumed to prefer the maximum depth of the domain. Swimming performance data of all three species showed no clear distinction between prolonged and burst swimming modes (Hoover et al., 2017; Peake et al., 1997) so all endurance calculations used a single set of parameters for unsustainable swimming. Table 1 provides the size range, maximum sustained swim speed, $U_{sus}$, and swimming performance curve coefficients of each species. Fish passage analyses were run for current gate operating conditions specified by the USACE Water Control Manual.

#### 2.3.3. Modelling fish passage under modified gate operating procedures

After evaluating theoretical passage of silver carp, bighead carp, and lake sturgeon during current gate operating procedures, we used the model to evaluate whether and how modifications to gate operating procedures might further impede bigheaded carp passage while at the same time minimally impacting scour protection and lake sturgeon passage. Because our evaluation of current gate operating procedures found that they were producing a previously unknown and unexpected imbalance in flow through the gates, a new set of gate operating procedures were sought. The modified gate operating procedures were set to correct the flow imbalance and produce uniform velocity distributions downstream of the dam that were also less than the maximum allowable velocity at the endsill for scour protection set by the USACE of 1.5 m/s. This was accomplished with modest modifications to gate operating procedures, less than 0.6 m difference on average in gate opening height from current operating procedures in the USACE Water Control Manual (See Table 2 for changes in gate opening heights). Fish passage analyses were run for the modified gate operating procedures using the same number of individuals, length distributions, and swimming performance metrics as the analysis of current gate operations. The efficacy of the modified gate operations to block silver carp and bighead carp was determined by comparing the modified passage results with current passage.

**Table 1**
Size range and swimming performance characteristics for silver and bighead carp (Hoover et al., 2017) and lake sturgeon (Peake et al., 1997) used in Eq. (7).

| Species | Total length (mm) | $U_{sus}$ (TL/s) | a (mean ± $\sigma_a$) | b (mean ± $\sigma_b$) |
|---|---|---|---|---|
| Silver carp | 600–1000 | 1.25 | 1.92 ± 0.65 | −1.02 ± 0.33 |
| Bighead carp | 700–1100 | 1.00 | 5.52 ± 0.73 | −2.98 ± 0.41 |
| Lake sturgeon | 900–1300 | 0.75 | 11.03 ± 0.82 | −8.44 ± 0.70 |

**Table 2**
Changes in gate opening height and depth-averaged velocities calculated from the CFD model at the endsill of the tainter and roller gate sections under current and modified gate operating procedures. The maximum allowable velocity at the endsill by the USACE Water Control Manual is 1.5 m/s. Velocity calculations for modified gate operation at 625 $m^3$/s reflects conditions where two roller gates are completely closed.

| Discharge ($m^3$/s) | Tainter Gate | | | Roller Gate | | |
|---|---|---|---|---|---|---|
| | Current velocity (m/s) | Avg. change in opening (m) | Modified velocity (m/s) | Current velocity (m/s) | Avg. change in opening (m) | Modified velocity (m/s) |
| 625 | 0.6 | +0.12 | 1.0 | 0.8 | −0.40* | 1.0 |
| 1250 | 0.8 | +0.14 | 1.0 | 1.2 | −0.12 | 1.1 |
| 1475 | 0.9 | +0.20 | 1.2 | 1.4 | −0.15 | 1.2 |
| 2325 | 1.4 | +0.24 | 1.8 | 2.1 | −0.24 | 1.8 |
| 2720 | 1.5 | NA | NA | 1.6 | NA | NA |

NA – Not applicable, all gates are out of the water at 2720 $m^3$/s.
* Change in gate opening height averaged across the 3 open roller gates.

#### 2.3.4. Statistical analysis of fish passage

The passage index, an estimate of the maximum percentage of a theoretical distribution of fish from each size class to pass was calculated by dividing the total number of successful passages by the total number of individuals. Passage index data for each size class were calculated according to Eq. (12) and binned into 10 equal sized groups to obtain the mean ± S.D. passage index ($PI_{TL}$) across the group. Within each sub-group, the passage index is calculated as

$$PI_{TL} = \frac{Count\ of\ fish\ passed\ of\ size\ TL}{Total\ of\ fish\ seeded\ into\ model\ of\ size\ TL} \quad (12)$$

where each individual size class is designated by total length (TL). Student's t-tests (equal variance, two-sided) were used to test whether the mean passage index of a specific size class differed between current

and modified conditions. Next, population scale passage index ($PI_{pop}$) values were calculated by summing the products of the percent frequency (%Pop) of each size class from species specific size distribution by the size specific passage index as demonstrated by Eq. (13).

$$PI_{pop} = \sum_{i}^{TL} (PI_i * \%Pop_i) \quad (13)$$

The population scale passage index was calculated across the 10 sub-groups and student's t-tests (equal variance, two-sided) were used to test whether the mean passage index of a population differed between current and modified conditions. For both analyses, values were examined for normalcy (Shapiro-Wilk tests). All analyses were conducted with custom scripts in Matlab (Mathworks, MA, USA). Significance was determined at $p < 0.05$.

#### 2.3.5. Sensitivity analysis

Lastly, a sensitivity analysis was performed to demonstrate that the model configuration used in our analysis resulted in the most conservative estimates of fish passage index and to understand how the stochastic features of the model (swimming performance, turbulence representation, and path selection method) might impact results. This was performed in lieu of a traditional validation because bigheaded carp are so uncommon at this location as to be uncatchable and no data are available to relate bigheaded carp passage through individual lock-and-dam gates. Sensitivity analyses were conducted about a base condition using the results of the base model for 5000 silver carp with a body length of 800 mm during current gate operations at 2325 $m^3/s$. The sensitivity analysis was run for silver carp during a single discharge and gate operation condition because the impacts of the stochastic model features are conserved across all flow and gate operating conditions, fish species, and total length. First, we evaluated the impact of swimming performance metrics on model results by doubling maximum fatigue (i.e., fatigue occurs at 200%) and then by reducing the maximum fatigue by half (i.e., fatigue occurs at 50%). Next, we examined the impact of turbulent velocity fluctuations by using the steady state velocity field, thereby allowing fish to move through a static flow field. Another model examined the impact of variation in swimming performance metrics by using only the mean swimming performance metrics (Section 2.2.1) (Table 1) for all individuals. Finally, to ensure our fatigue based pathway selection method differed from a simple random walk, we ran a model using the same swimming performance metrics and turbulent fluctuations approaches as our base model with step selection following a purely biased random walk.

## 3. Results

### 3.1. Passage under current USACE gate operating procedures

Model runs of our agent-based model under current operating procedures indicated that there are flow imbalances across Lock-and-Dam #8, with low velocity regions that all fish could be exploiting to pass without exhausting (Fig. 6A and B). CFD simulations revealed that the low velocity regions were caused by areas of rotational flow and an imbalance in discharge through the tainter and roller gates at all flow conditions. Flow rates through each gate type differed by as much as 27% from those expected in the Water Control Manual (USACE, 2003). The water volume ratio of flow through the tainter and roller gates was 39:61 across all discharges. Depth-averaged velocities downstream of the roller gates exceed the USACE maximum allowable velocity of 1.5 m/s (Table 2). Deceleration of flows downstream of the dam under current operating procedures also creates two zones of horizontal rotating flow along both banks and a third zone of vertical rotational flow in a downstream scour hole.

The passage index of both silver and bighead carp under all flows and current operating procedures was proportional to fish length, with larger fish groups having a higher passage index than small fish (Fig. 7). The population scale passage index (i.e., maximum percentage of a theoretical distribution of fish to pass) for silver and bighead carp populations ranged from 2 to 12% and 0-4%, respectively (Table 3) across all flow conditions. The highest passage indices of either species occurred for silver carp during both open-river, 2720 $m^3/s$, and the lowest modeled discharge, 625 $m^3/s$. While high values of passage index were expected for open-river conditions, when velocities at the structure are lowest, similarly high index values at the lowest discharge, when velocities are highest, were unexpected. Close inspection of silver carp trajectories through a tainter gate opening revealed it was possible to avoid the high velocity jet created by the narrow gate opening by utilizing regions of relatively slow and reversed flow caused by the stepped spillway and recirculating flows near the water surface (Fig. 8A).

Results of the agent-based model also indicated lake sturgeon passage during current gate operating procedures was relatively constant across all flows (Table 3), ranging from 2 to 6%. Similar to the silver carp, lake sturgeon that passed through the dam did so through the outermost gates (Fig. 6E and F). The specified tendency of lake sturgeon to swim on the bottom resulted in pathways that shifted laterally in front of the roller gates as demonstrated by the increased line density near the roller gates in Fig. 6E and F, a feature not observed in either silver or bighead carp. Although silver and bighead carp have superior swimming performance compared to lake sturgeon relative to body length (Table 1), lake sturgeon (median TL ~ 1000 mm) can obtain similar absolute swim speeds as bighead carp (median TL ~ 700 mm) due to their large size.

### 3.2. Passage under modified gate operating procedures

Gate operating procedures in the model were modified to match a constant water volume ratio of 45:55 through the tainter and roller gates, respectively, to mitigate the predicted high velocities downstream of the roller gates under current conditions. This would result in modest modifications to gate operating procedures (see Table 2) which the model predicted to produce near uniform velocity distributions downstream of the dam, while also seemingly minimizing regions silver carp and bighead carp could exploit (Fig. 9 and Supplementary Fig. 15). Although the proposed modifications do not eliminate zones of rotational flow, velocities are redistributed across the dam which minimized regions of low velocities. The modifications caused an increase in depth-averaged velocity below the tainter gates while decreasing the depth-averaged velocities below the roller gate openings (Table 2). Although the depth-average velocity at 2325 $m^3/s$ still exceeded the maximum allowable velocity set by the USACE of 1.5 m/s, the velocity at the roller gate was reduced from 2.1 m/s to 1.8 m/s. No incremental increase in scour around the dam was expected since the average velocities under modified gate operating procedures do not exceed current conditions.

Results of the agent-based model indicated that both silver and bighead carp passage would be reduced during all flow conditions during modified gate operating procedures (Table 3). Silver carp passage was reduced by over 50% from current conditions (t-test: $p < 0.05$) (Table 3) at discharges greater than 1250 $m^3/s$, while bighead carp passage was found to decrease at all flows but 1250 $m^3/s$ (t-test: $p < 0.05$). Further, bighead carp passage was reduced to nearly zero at 1475 and 2325 $m^3/s$. While uniform modifications to gate operation at 1250 $m^3/s$ increased the silver carp passage index slightly, the overall index remained below 5% and the bighead carp passage index was unchanged (Table 3). At the lowest river discharge, 625 $m^3/s$, a second modification case was considered because flow spread across all gates and minimally reduced passage of both bigheaded carp species (Fig. 7A, C and E). To reduce carp passage, flow had to be further restricted by closing the two outside roller gates (flow distributed across all tainter gates and 3 of 5 roller gates) (Figs. 8B and 9A,

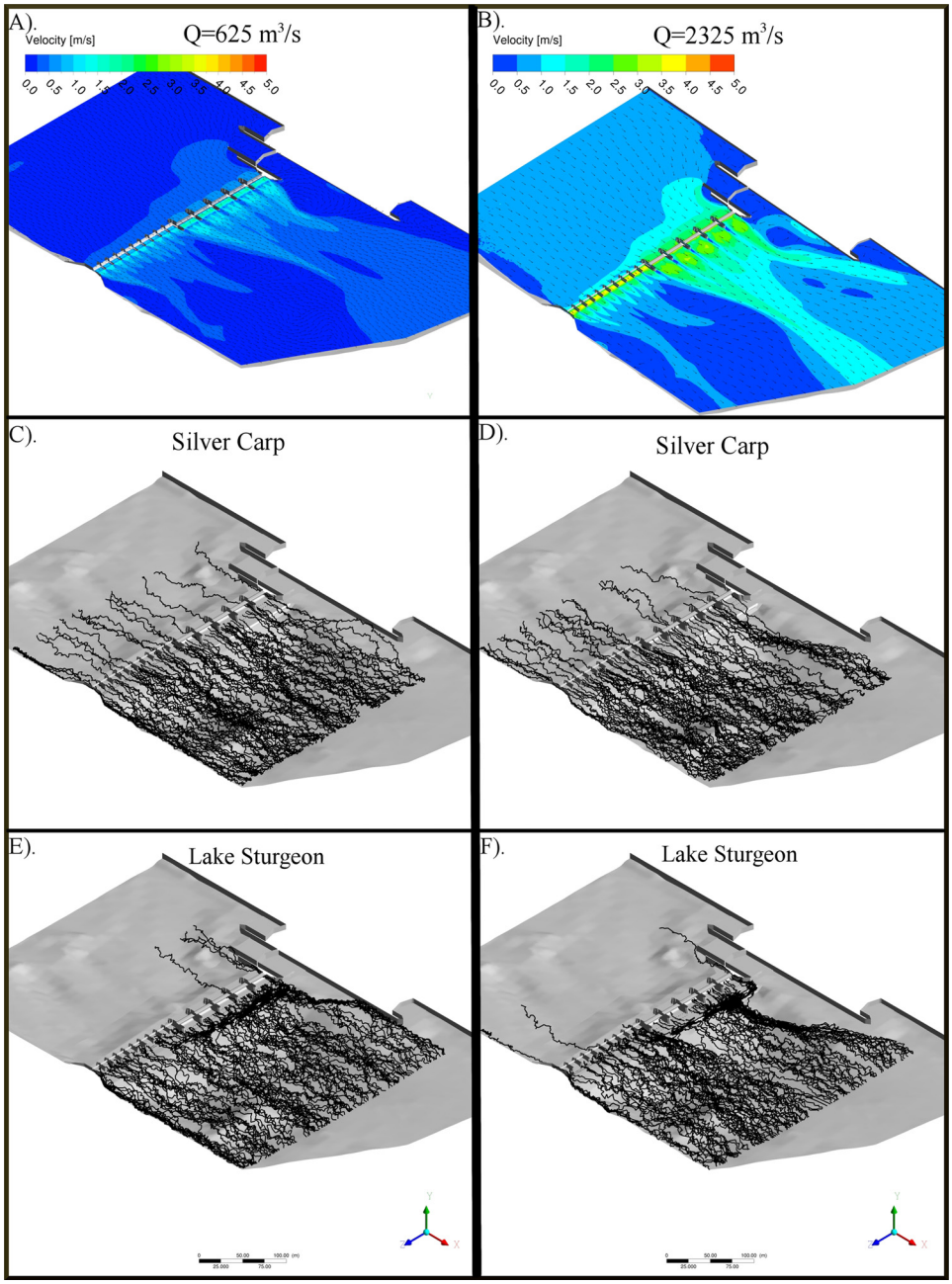


**Fig. 6.** Velocity magnitude contours at a plane 1 m below the tailwater surface level during a river discharge 625 $m^3$/s (A) and 2325 $m^3$/s (B) at Lock-and-Dam #8 under current gate operations. River flow is moving left to right. Simulated swimming paths of 100 silver carp (C and D) and 100 lake sturgeon (E and F) are shown for each condition. See Supplemental Figs. 17 and 18 for enlarged velocity contour map with vector fields and Supplemental Fig. 14 for swimming paths of 100 bighead carp.

and Supplementary Fig. 19). This modification produced velocity conditions similar to the current operation for a discharge of 1250 $m^3$/s, and reduced the silver carp passage index by 76% (t-test, $p < 0.01$) (Table 3). In general, this low flow modification increased velocities in the center of the river and alters the shape of the recirculation zones (Fig. 9A). An analysis of outdraft conditions (i.e., flow capable of pulling barges away from the lock approach and towards the spillway gates) during river discharge of 625 $m^3$/s indicated modified gate operations should not impact navigation, as nearly no change in velocity or direction of flow is expected (See Supplementary Fig. 16).

The passage index of lake sturgeon decreased during modified gate operations only for 625 $m^3$/s (t-test: $p < 0.05$) (Table 3). While not significant, the lake sturgeon passage index increased under all remaining discharges. Passage of lake sturgeon was not strongly related to total length; under 625 $m^3$/s the range of passage index for all size classes was between 0–5% (Fig. 7E and F). Although somewhat diminished compared to current operations, lake sturgeon pathways still exhibited significant lateral movement downstream of the roller gates under modified gate operating procedures as demonstrated by the increased line density near the roller gates in Fig. 9E and F.

### 3.3. Sensitivity analysis

There were significant differences observed in the passage index between model variants (Fig. 10). Although repeated measures ANOVA indicated that the passage index was not sensitive to a two-fold increase in total fatigue, a two-fold decrease significantly decreased passage. Comparisons between the two stochastic parameters suggested variable

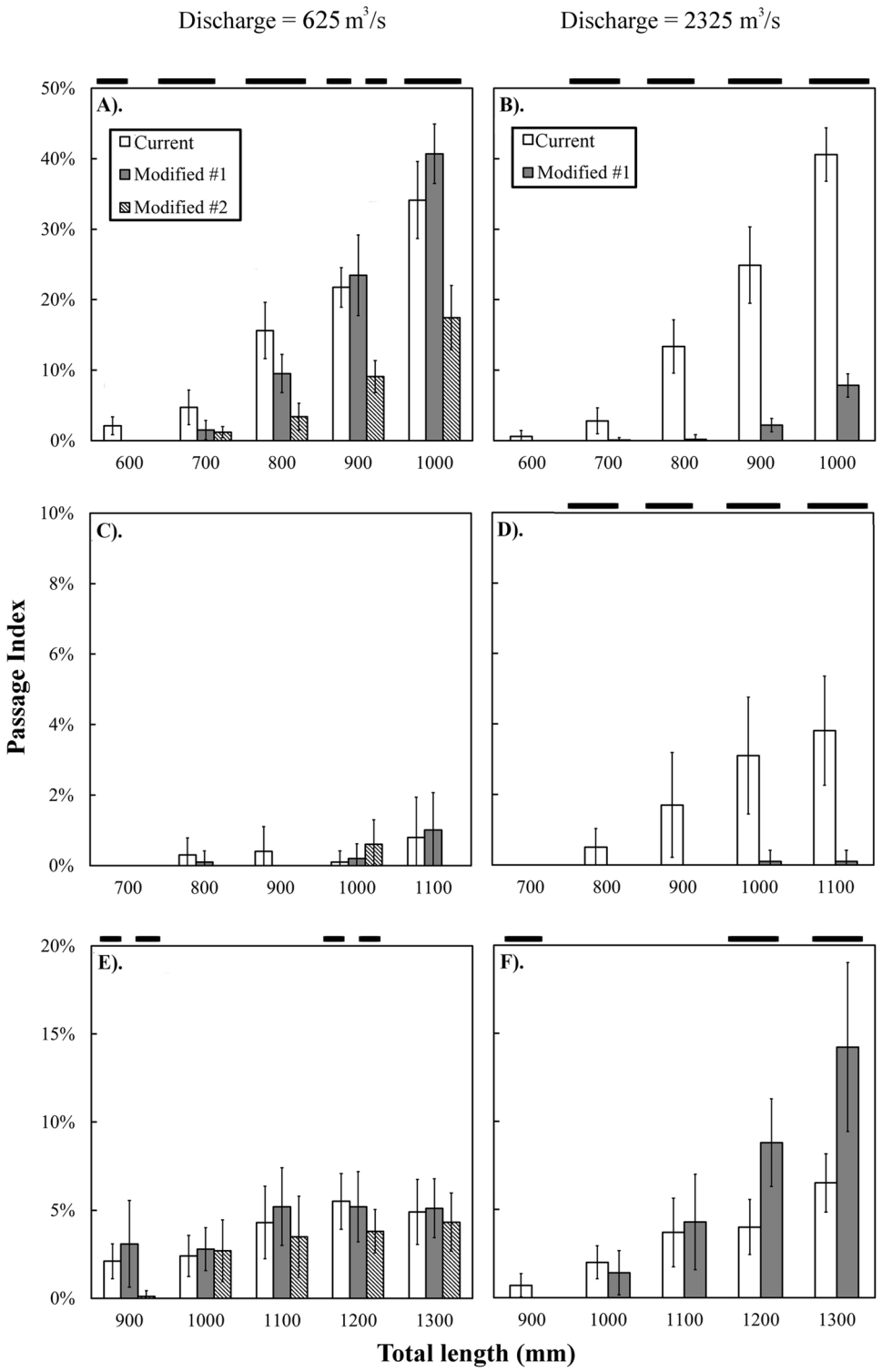


**Fig. 7.** Mean passage index ± S.D. of silver carp (A and B), bighead carp (C and D), and lake sturgeon (E and F) at each size class for river discharges of 625 $m^3/s$ and 2325 $m^3/s$ during current (white bar) and modified gate operations (grey and hatched bars). At 625 $m^3/s$ two cases of modified gate operation were considered: (1) all gates used to evenly distribute flow (grey bar) and (2) reduced gate usage (2 of 5 roller gates closed) (hatched bar). Statistical significance of $p < 0.05$ from *t*-tests between current and modified cases are denoted by a black bar. Note change in ordinate axis.

swimming performance parameters have greater influence on passage indices than does velocity fluctuations. As expected, our fatigue based pathway selection method generated a significantly higher passage index than that resulting from a random walk process.

## 4. Discussion

In this paper, we introduce and describe a novel agent-based approach built on the physiological limits of fish swimming performance as a broadly applicable fish passage model to estimate fatigue in fish swimming upstream in complex flows, like those present around lock-

**Table 3**
Mean ± S.D. population scale passage index at modeled river discharges for silver carp, bighead carp, and lake sturgeon under current and modified gate operating procedures (n = 5000 each species per flow). At river discharge 625 $m^3/s$ modified case C1 distributed flow across all gates while modified case C2 distributed flow across gates 1–13. Student's *t*-test comparison between current and modified passage indices determined p-value, $p < 0.05$ indicates a significant change in mean value.

| Species | River discharge ($m^3/s$) | | | | |
|---|---|---|---|---|---|
| | 625 | 1250 | 1475 | 2325 | 2720 |
| Silver carp | | | | | |
| Current (%) | 10.6 ± 3.2 | 1.3 ± 1.0 | 3.7 ± 2.0 | 8.6 ± 2.8 | 11.3 ± 4.7 |
| Modified (%) | C1: 6.5 ± 2.1 C2: 2.4 ± 1.3 | 2.5 ± 1.6 | 1.8 ± 1.6 | 0.2 ± 0.5 | NA |
| p-value | C1: < 0.01 C2: < 0.01 | 0.03 | < 0.01 | < 0.01 | NA |
| Bighead carp | | | | | |
| Current (%) | 0.1 ± 0.2 | 0.1 ± 0.1 | 0.1 ± 0.1 | 0.6 ± 0.4 | 3.6 ± 1.1 |
| Modified (%) | C1: 0.1 ± 0.1 C2: 0.0 ± 0.1 | 0.0 ± 0.1 | 0.0 ± 0.0 | 0.0 ± 0.0 | NA |
| p-value | C1: 0.09 C2: 0.01 | 0.12 | 0.01 | < 0.01 | NA |
| Lake Sturgeon | | | | | |
| Current (%) | 3.0 ± 1.3 | 2.4 ± 1.4 | 2.5 ± 1.3 | 2.3 ± 1.1 | 6.4 ± 2.0 |
| Modified (%) | C1: 3.5 ± 1.8 C2: 2.2 ± 1.3 | 2.7 ± 1.5 | 2.9 ± 1.8 | 3.0 ± 1.5 | NA |
| p-value | C1: 0.11 C2: 0.01 | 0.47 | 0.29 | 0.10 | NA |

NA – Not applicable, all gates are out of the water at 2720 $m^3/s$.

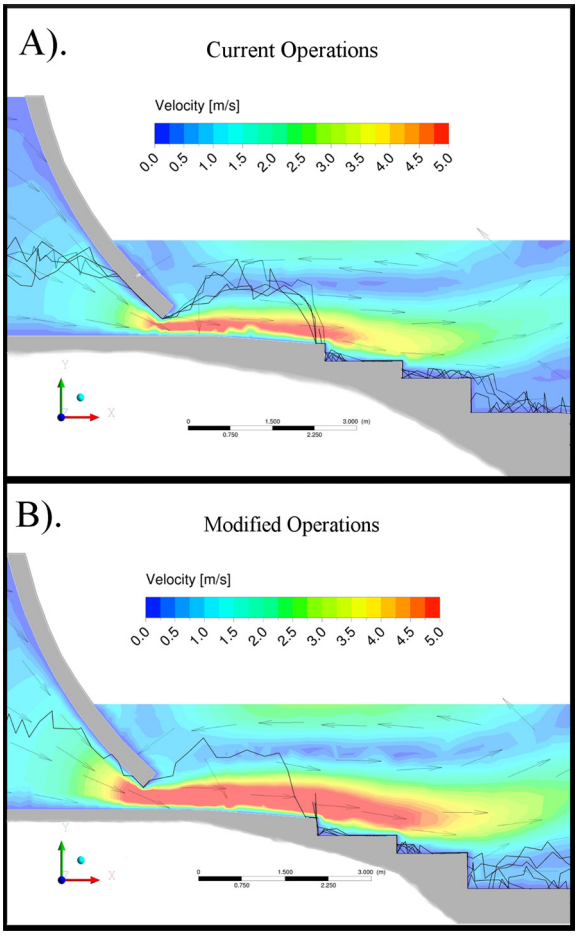


**Fig. 8.** Cross-sectional velocity magnitude contours, vector field, and sample silver carp swimming paths through a tainter gate bay during a discharge of 625 $m^3/s$, at Lock-and-Dam #8 during current (A) and modified, C2, (B) gate operations. Terminated swimming paths indicate fish that completely fatigued. River flow is moving left to right in each image. The difference between current and modified operations is the distribution of velocities upstream of the tainter gate (curved grey object) and gate opening.

and-dams. Our approach is novel because it computes the highest possible number of fish from a given population to pass a hydraulic challenge by forcing simulated fish to swim upstream and seek a path of least fatigue. Model results are considered conservative (i.e. they likely overestimate fish passage) from the perspective of invasive species control for which managers seek ways to reduce passage and do not want to underestimate passage as it would have devastating consequences. Importantly, our model operated independently of fish behavioral data, which can be hard to come by for newly invading species and do not yet exist for bigheaded carps. We demonstrated the value of the model by simulating the potential passage of invasive bigheaded carp through a typical lock-and-dam in the Mississippi River and found modifications to gate operating procedures that should decrease passage.

Importantly, we found that very modest modifications to gate operation, which accomplish the USACE goal of evenly distributing velocities across the dam, can further reduce passage of bigheaded carp without seemingly impacting lake sturgeon passage. Modeling flow and fish passage in three-dimensions highlights the importance the distribution of velocities through an opened gate plays on fish passage at Mississippi River lock-and-dams. Initial attempts to correlate fish passage to gate operation used depth averaged velocities only to suggest fish were unlikely to pass through the dams when the head differential was > 1 m (i.e., low river discharge) (Zigler et al., 2004); however, Tripp et al. (2014) recently found that aside from open-river conditions, the majority of fish passages observed in the lower Mississippi River occurred at ≥ 1 m head differential. Our model also found that silver carp passage peaked at 10% when the river discharge was 625 $m^3/s$ and the head differential was 2.6 m. Increased passage can be attributed to fish being able to avoid high velocity jets through gate openings by utilizing adjacent regions of slow and reversed flow caused by the stepped spillway and recirculating flows near the water surface (Fig. 8). We found that restricting flow across fewer gates at low discharge eliminates this weakness. Conventional fish passage models using depth and time averaged velocities would not have identified this condition because of their inability to resolve such fine flow details.

The low passage rates of carp predicted by our model at Lock-and-Dam #8 are very consistent with (and may explain) the low number of bigheaded carp captured in the Upper Mississippi River. For instance, over the past 21 years, only 33 bigheaded carp have been captured upstream of Lock-and-Dam #8 (USGS Nonindigenous Aquatic Species database). Remarkably low passage rates of acoustically tagged bigheaded carp have also been described at the Starved Rock Lock-and-Dam on the Illinois River (13 of 153 detected below the dam passed

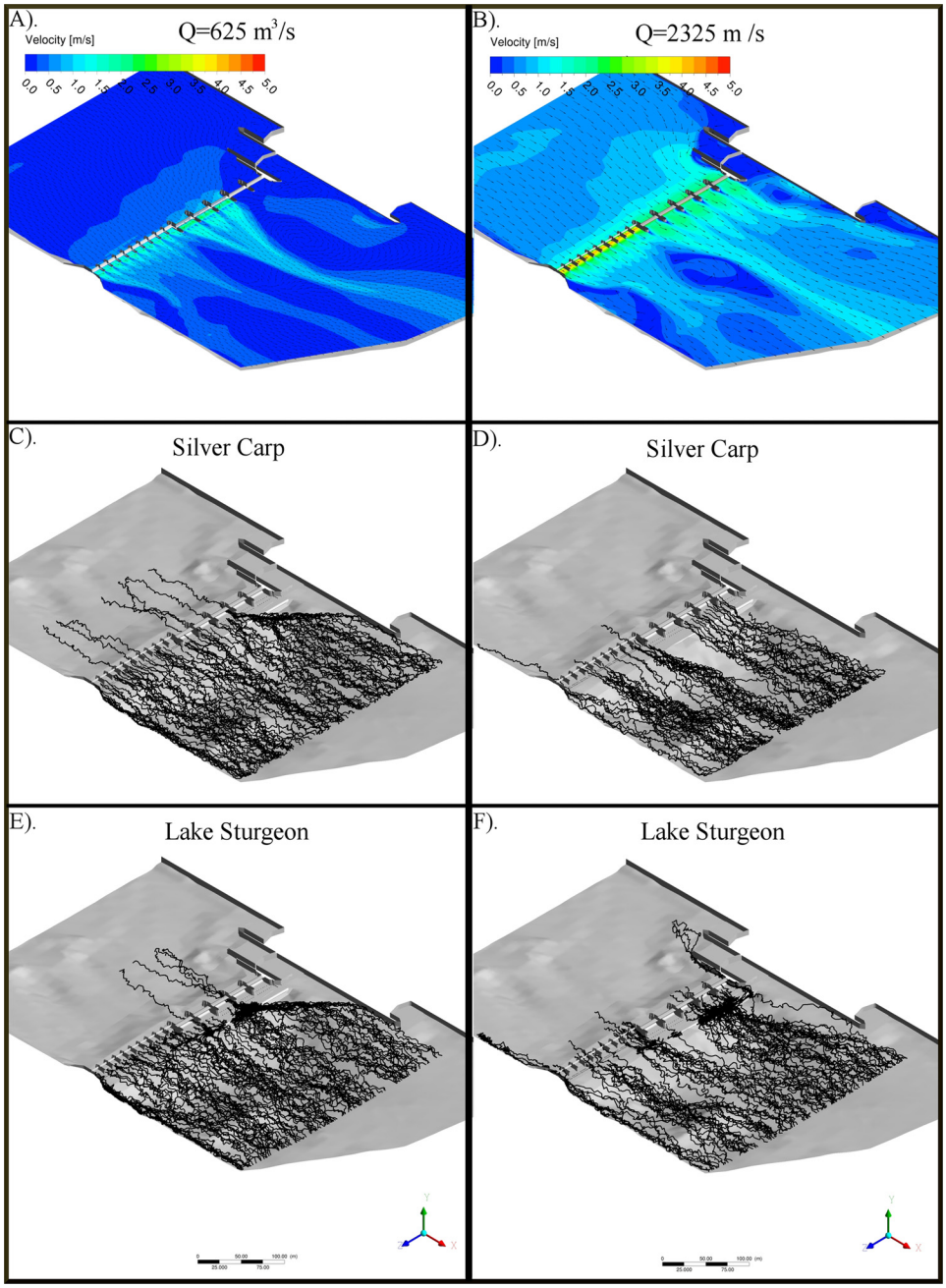


**Fig. 9.** Velocity magnitude contours at a plane 1 m below the tailwater surface level during a river discharge 625 $m^3$/s (A) and 2325 $m^3$/s (B) at Lock-and-Dam #8 under modified gate operations. River flow is moving left to right. Simulated swimming paths of 100 silver carp (C and D) and 100 lake sturgeon (E and F) are shown for each condition. The modified gate operation in A re-distributes flow across 13 of 15 gates while the case shown in B uses all 15 gates (see Table 2). See Supplemental Figs. 19 and 20 for enlarged velocity contour map with vector fields and Supplemental Fig. 15 for swimming paths of 100 bighead carp.

upstream over 3 years) (Lubejko et al., 2017) and between Lock-and-Dam #20-26 on the Mississippi River (63 of 320 detected at any of the 6 dam s passed upstream over 4 years) (Tripp et al., 2014). Consistent with previous tagging studies, our model predicts most passages would occur during open-river. An ongoing telemetry study of common carp, Cyprinus carpio, passage at Lock-and-Dam #2 on the Mississippi River has also observed no successful passages through spillway gates, an observation reinforced by preliminary runs of this model at Lock-and-Dam #2 (Finger et al., unpublished data).

Our assertion that the model overestimates fish passage rates draws support from three lines of evidence. First, the model assumes all fish will swim continuously upstream, without backtracking. This assumption represents an extreme condition because not all fish will try to pass a hydraulic challenge (Bunt et al., 1997; Haro et al., 2004; Castro-Santos, 2004). In the case of silver carp, Coulter et al. (2016) found that 15–30% of tagged individuals moved downstream during March and April in an unregulated river, when fish were expected to move upstream to spawn. Second, the model assumes fish are able to instantaneously adjust their swim speed to maintain the distance-maximizing ground speed. Not only does this assumption lead to fish swimming the absolute maximum distance possible, but instantaneous adjustments to swim speed result in simulated accelerations that are unrealistically high. In nature, the forward acceleration of a fish is determined by the balance of forces acting on the fish (i.e., friction, local velocities, and pressure) and thrust generated by locomotion. Even in simplified hydraulic conditions with uniform velocities, Castro-

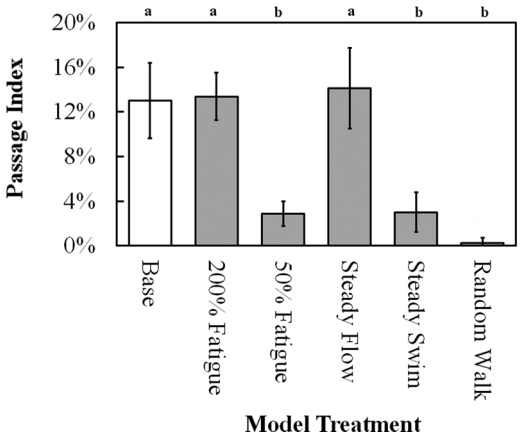


**Fig. 10.** Sensitivity of agent-based model to variations in maximum fatigue level, stochastic representation of flow and swimming ability, and random movement. All cases ran 1000 silver carp (TL = 800 mm) under historic gate operations during a river discharge of 2325 $m^3/s$. Results presented as mean ± S.D. passage index. Different letters above bars indicate significant differences between groups using a Tukey HSD post hoc comparison ($p < 0.05$).

Santos (2005) observed only one of six species (anadromous clupeids) swam at their distance maximizing ground speed. Third, the model assumes fish follow the path of least fatigue and swim continuously until they completely exhaust. This assumption likely leads to overestimates of passage because real fish may terminate unsustainable swimming efforts prior to complete exhaustion (Castro-Santos, 2005; Peake and Farrell, 2006). Fish may stop short of complete exhaustion to stage multiple passage attempts (Castro-Santos, 2005) or facilitate intermittent locomotion (i.e., fish exploit favorable hydraulic conditions to alternate unsustainable swimming efforts with periods of rest without losing ground) (Kramer and McLaughlin, 2001). While the model accounts for fish exploiting favorable hydraulic conditions through use of the resultant velocity, periods of rest are not explicitly considered. To address this potential issue, we used the sensitivity analysis to examine a similar situation where fish are given a two-fold increase in their time-to-fatigue. This case is akin to fish swimming to exhaustion, immediately recovering without losing ground, and swimming to exhaustion again. The fact increased time-to-fatigue did not significantly increase the passage index (Fig. 10), lends greater support to our assumption that the path of least fatigue is analogous to pathways generated from multiple passage attempts.

Although integrating hydraulics with swimming performance in a numerical model that predict upstream fish passage is not a new concept, it has had limited application. For example, FishXing (developed in the late 1990s) has become a common software package used by fish passage practitioners (Furniss et al., 2006), even though it relies on overly simplified representations of flow (e.g., 1-D hydraulic models) and assumes swimming performance is constant for all fish of a given species. These simplifications can result in conservative estimates of fish passage which can lead to designs with limited biological benefit (Mahlum et al., 2014; Furniss et al., 2006). More robust models pairing steady state, three-dimensional flow simulations with fish energetics have been used in contemporary analyses of fishway designs (Khan, 2006; Khan et al., 2008). However, these models only consider two or three prescribed movement paths meant to capture the range of conditions fish are expected to encounter. This restriction of movement pathways essentially devolves the model to a one-dimensional problem. Arguably the most robust fish movement model is the Eulerian-Lagrangian-agent method (ELAM) developed by Goodwin et al. (2006, 2014). The ELAM forecasts fish movements in novel conditions using behavioral decision making algorithms that relate fish movements to water accelerations. However, while the ELAM has been successful at describing mechanisms governing downstream migrating salmon (Goodwin et al., 2014), it requires large telemetry data sets to formulate and test the behavioral rules. Using a mechanistic approach, Arenas et al. (2015) also pairs high-resolution CFD output with large telemetry data sets (401 fish tracked with 63,465 positions) to characterize fish behavior in responses to hydraulic conditions. Unfortunately, such data sets are lacking for many species, including invasive fish like bigheaded carp, and upstream passage at dams in general. Moreover, behavior-based fish passage models like those developed by Haefner and Bowen (2002) and Goodwin et al. (2006, 2014) minimize the influence of swimming fatigue as they were intended to describe downstream movement of juvenile Pacific salmon. This is a crucial feature since upstream movement through hydraulic challenges requires significant unsustainable swimming efforts, whereas it is primarily used to avoid obstacles when swimming downstream.

Modelled fish pathways emerged through discrete decisions made by individual fish based on physiological attributes and local velocity fields. The pathways were unique to each simulated fish due to the introduction of physical (e.g., turbulence fluctuations) and biological variation (e.g., swimming performance parameters, size, starting point). The requirement of fish to seek the pathway of least fatigue manifested in routes that tended to move along shorelines and structure boundaries and concentrated near areas of low velocity / high friction (Figs. 6, 8, and 9). This phenomenon appears consistent with the reduced-velocity zone hypothesis which states fish accomplish upstream movements through culverts via pathways in low-velocity, low turbulence boundary layers (Johnson et al., 2012, Powers et al., 1997). Despite no explicit link to fish behavior and vastly different hydraulic conditions, the fact our simplified model simulated pathways that are similar to coho salmon (Oncorhychus kisutch) and brook trout (Salvelinus fontinalis) passing through corrugated culverts (Johnson et al., 2012; Goerig et al., 2016) reinforces the hypothesis that successful upstream passage at lock-and-dams has strong dependence on swimming ability. Regardless, linking movement decisions to observed behaviors of fish in situ would further enhance model utility and should be sought for future installments of the model.

The sensitivity analysis demonstrated that modifications to our base assumptions (including a two-fold increase in time-to-fatigue) do not produce higher estimates of fish passage. The comparison between the two stochastic features of the model (e.g., turbulence and swimming performance metrics) revealed that swimming parameters accounts for more variation in the model than a fluctuating velocity field. This may indicate that uncorrelated velocity fluctuations used here may offer little improvement over steady state velocity conditions, and exact simulations of correlated velocity fluctuations are needed. An alternative explanation of the low impact of turbulent fluctuations may be the minimal turbulence in areas the fish frequented. Since the model sought zones of least fatigue, fish would presumably avoid regions where the turbulent fluctuations would be greatest (i.e., chance for high instantaneous velocity), thus reducing its influence on passage index. Further examination of unsteady flow statistics on fish passage is required.

The resolution of the computational mesh limits the model because of its effects on CFD simulations and fish movement. Decisions on mesh size selection must balance the need for accurate simulations with the requisite computational resources. Our computational meshes contained elements with a side length (i.e., distance between nodes) between 0.15–1.5 m, which resulted in meshes containing nearly 2 million nodes and 12 million elements. These mesh parameters limit simulation of turbulence with a length-scale less than 0.15 m, which is still more than 3 times smaller than the smallest fish modeled. Regardless, there was good agreement between the CFD models and both field and laboratory velocity measurements, so the potential benefit of a finer mesh was not considered. Mesh resolution could also impact fish trajectories because fish were restricted to moving between nodes. We attempted to limit grid dependent paths by forcing simulated fish to examine 3 or

more nodes during each movement step (e.g., silver carp examined an average of 12 neighboring nodes at each step). Future improvements to the model should consider changes to the step selection process that minimizes mesh dependency (i.e., Lagrangian movement model).

Additionally, while selected lock-and-dam structures (#2, #5, and #8) are already anecdotally considered barriers to native fish passage in the Mississippi River (Zigler et al., 2003, 2004; Knights et al., 2002), alterations to their gate operating procedures could be studied using our model to perhaps improve passage, at least at certain times of the year. While the conservative assumptions of the model preclude any definitive conclusions on lake sturgeon passage, the results indicate that the opportunity for passage is not diminished by the proposed modifications. Further, lake sturgeon represents just one of over 100 Mississippi River species (Wilcox et al., 2004) and swimming performance data on other species is limited to < 10 species. Regardless, there is always the possibility for fish to pass a lock-and-dam by swimming through the navigational lock chamber. Although bigheaded carp do pass through lock chambers, the rate appears to be small (Lubejko et al., 2017; Tripp et al., 2014) and could be further reduced using behavioral deterrents, such as sound projectors, to guide fish towards the gated spillway (Noatch and Suski, 2012; Zielinski and Sorensen, 2016). These sound systems can be taxon specific as carp have an extraordinary sense of hearing (Zielinski and Sorensen, 2016). Generally, lock chambers are also not considered sustainable pathways for fish because they have minimal attraction flow and only operate intermittently with boat traffic (Wilcox et al., 2004).

Although our model provides immediate utility to invasive fish control, it could be improved. Recent advances in our understanding of fish swimming behavior (Otezia et al., 2017) could allow inclusion of fish behavior in the model, expanding on the fairly rigid movement rule-set currently employed (i.e., fish only swim upstream). Similarly, fish behavior is not just influenced by flow alone, it can be influenced by other environmental stimuli (e.g., temperature, light, sound, predators), and further study is needed to understand how to account for these factors computationally. Adding these data would be especially useful for native fish.

## 5. Conclusions

We describe and test a novel agent-based fish passage model that can now be used to guide efforts to slow the upstream migration of non-native invasive species whose behavior is not yet understood and that may be easily and safely implemented. Our findings show the utility of a novel computational tool to identify and potentially modify hydraulic conditions to benefit fish passage or control. The agent-based approach offers robust opportunity to test how different physiological characteristics (i.e., fish with improved swimming performance) could influence overall passage and is a critical first step in predicting passage of fish through hydraulic challenges. In particular, at Lock-and-Dam #8, we found that current gate operations inhibit bigheaded carp passage and that modest operational modifications could enhance this feature. Such modifications could be implemented quickly, at little to no cost, and seemingly would not interfere with the navigational function of lock-and-dams (See Supplemental Fig. 16). Due to the possibility of improving velocity distributions downstream of the dam and the ancillary benefit of limiting upstream passage of invasive species, the USACE is now evaluating the potential to implement these gate operating procedures on a trial basis. Although gate operations alone cannot block all bigheaded carp in the Mississippi River, the modifications offer a management tool that could minimize passage of bigheaded carp to delay or possibly prevent establishment of populations upstream. This approach could also be exported to other applications that require an improved understanding of fish fatigue such as fishway design or identification of barriers to migration and dispersal.

## Acknowledgements

This study was funded by the Minnesota Environmental and Natural Resources Trust Fund as recommended by the Legislative-Citizen Commission on Minnesota Resources (LCCMR). The authors acknowledge the Minnesota Supercomputing Institute (MSI) at the University of Minnesota and Institute for Cyber-Enabled Research at Michigan State University for providing resources that contributed to the research results reported within this paper. We also thank the St. Paul District of the U.S. Army Corps of Engineers for their general assistance and detailing of lock-and-dam operations.

## Appendix A. Supplementary data

Supplementary material related to this article can be found, in the online version, at doi: https://doi.org/10.1016/j.ecolmodel.2018.05.004.

## References

Arenas, A., Politano, M., Weber, L., Timko, M., 2015. Analysis of movement and behavior of smolts swimming in hydropower reservoirs. Ecol. Mod. 312, 292–307.
Beamish, F.W.H., 1978. Swimming capacity. In: In: Hoar, W.S., Randall, J.D.Z. (Eds.), Fish Physiology: Locomotion, vol. 7 Academic Press Inc..
Bunt, C.M., Katopodis, C., McKinley, R.S., 1997. Attraction and passage efficiency of white suckers and smallmouth bass by two Denil fishways. N. Am. J. Fish. Manage. 19, 793–803.
Carlson, B.R., Propst, D.B., Stynes, D.J., Jackson, R.S., 1995. Economic Impact of Recreation on the Upper Mississippi River System. Technical Report EL-95-16. US Army Engineer Waterways Experiment Station, pp. 45.
Castro-Santos, T., 2004. Quantifying the combined effects of attempt rate and swimming capacity on passage through velocity barriers. Can. J. Fish. Aquat. Sci. 61, 1602–1615.
Castro-Santos, T., 2005. Optimal swim speeds for traversing velocity barriers: an analysis of volitional high-speed swimming behavior of migratory fishes. J. Exp. Biol. 208, 421–432.
Castro-Santos, T., 2006. Modeling the effect of varying swim speeds on fish passage through velocity barriers. Trans. Am. Fish. Soc. 135, 1230–1237.
Coulter, A.A., Bailey, E.J., Keller, D., Goforth, R.R., 2016. Invasive silver carp movement patterns in the predominately free-flowing Wabash River (Indiana, USA). Biol. Inv. 18, 471–485.
Daraio, J.A., Weber, L.J., Newton, T.J., Nestler, J.M., 2010. A methodological framework for integrating computational fluid dynamics and ecological models applied to juvenile freshwater mussel dispersal in the Upper Mississippi River. Ecol. Model. 221, 201–214.
FishPro Consulting Engineers and Scientists, 2004. Feasibility Study to Limit the Invasion of Asian Carp into the Upper Mississippi River Basin. Prepared for the Minnesota Department of Natural Resources and the U.S. Fish and Wildlife Service. .
Furniss, M., Love, M., Firor, S., Moynan, K., Llanos, A., Guntle, J., Gubernick, R., 2006. FishXing: Software and Learning Systems for Fish Passage Through Culverts, Version 3.0. U.S. Forest Sevice. San Dimas Technology and Development Center, San Dimas, California.
Gao, Z., Andersson, H.I., Dai, H., Jiang, F., Zhao, L., 2016. A new Eulerian-Lagrangian agent method to model fish paths in a vertical slot fishway. Ecol. Eng. 88, 217–225.
Ge, L., Sotiropoulos, F., 2005. 3D unsteady RANS modeling of complex hydraulic engineering flows. I: numerical model. J. Hydr. Eng. 131, 800–808.
Goerig, E., Castro-Santos, T., Bergeron, N.E., 2016. Brook trout passage performance through culverts. Can. J. Fish. Aquat. Sci. 73, 94–104.
Goodwin, R.A., Nestler, J.M., Anderson, J.J., Weber, L.J., Loucks, D.P., 2006. Forecasting 3-D fish movement behavior using a Eulerian-Lagragian-agent method (ELAM). Ecol. Model. 192, 197–223.
Goodwin, R.A., Politano, M., Garvin, J.W., Nestler, J.M., Hay, D., Anderson, J.J., Weber, L.J., Dimperio, E., Smith, D.L., Timko, M.A., 2014. Fish navigation of large dams emerges from their modulation of flow field experience. Proc. Natl. Acad. Sci. U. S. A. 111, 5277–5282.
Haefner, J.W., Bowen, M.D., 2002. Physical-based model of fish movement in fish extraction facilities. Ecol. Model. 152, 227–245.
Haro, A., Castro-Santos, T., Noreika, J., Odeh, M., 2004. Swimming performance of upstream migrant fishes in open-channel flow: a new approach to predicting passage through velocity barriers. Can. J. Fish. Aquat. Sci. 61, 1590–1601.
Harvey, G.L., Clifford, N.J., 2009. Microscale hydrodynamics and coherent flow structures in rivers: implications for the characterization of physical habitat. Riv. Res. Appl. 25, 160–180.
Hoover, J.J., Zielinski, D.P., Sorensen, P.W., 2017. Swimming performance of adult silver and bighead carp. J. Appl. Ichth. 33, 54–62.
Huth, A., Wissel, C., 1992. The simulation of the movement of fish schools. J. Theor. Biol. 156, 365–385.
Johnson, G.E., Pearson, W.H., Southard, S.L., Mueller, R.P., 2012. Upstream movement of juvenile coho salmon in relation to environmental conditions in a culvert test bed. Trans. Am. Fish. Soc. 141, 1520–1531.

Khan, L.A., 2006. A three-dimensional computational fluid dynamics (CFD) model analysis of free surface hydrodynamics and fish passage energetics in a vertical-slot fishway. N. Am. Fish. Manage. 26, 255–267.
Khan, L.A., Roy, E.W., Rashid, M., 2008. Computational fluid dynamics modelling of forebay hydrodynamics created by a floating juvenile fish collections facility at the Upper Baker River Dam, Washington. Riv. Res. Appl. 24, 1288–1309.
Kieffer, J.D., 2000. Limits to exhaustive exercise in fish. Comp. Biochem. Physiol. Part A Mol. Integr. Physiol. 126, 161–179.
Knights, B.C., Vallazza, J.M., Zigler, S.J., Dewey, M.R., 2002. Habitat and movement of lake sturgeon in the upper Mississippi River system, USA. Trans. Am. Fish. Soc. 131, 507–522.
Kolar, C.S., Chapman, D.C., Courtenay Jr., W.R., Housel, C.M., Williams, J.D., Jennings, D.P., 2007. Bigheaded Carps: A Biological Synopsis and Environmental Risk Assessment. American Fisheries Society. Special Publication 33, Bethesda, MD.
Kramer, D.L., McLaughlin, R.L., 2001. The behavioral ecology of intermittent locomotion. Am. Zool. 41, 137–153.
Liao, J.C., Beal, D.N., Lauder, G.V., Triantafyllou, M.S., 2003. Fish exploiting vortices decrease muscle activity. Science 302 (5650), 1566–1569.
Lubejko, M.V., Whitledge, G.W., Coulter, A.A., Brey, M.K., Oliver, D.C., Garvey, J.E., 2017. Evaluating upstream passage and timing of approach by adult bigheaded carps at a gated dam on the Illinois River. River Res. Appl. 1–11. http://dx.doi.org/10.1002/rra.3180.
Mahlum, S., Cote, D., Wiersma, Y.F., Kehler, D., Clarke, K.D., 2014. Evaluating the barrier assessment technique derived from FishXing software and the upstream movement of brook trout through road culverts. Trans. Am. Fish. Soc. 143, 39–48.
Markussen, J.V., Wilhelms, S.C., 1987. Scour Protection for Lock and Dams 2-10, Upper Mississippi River. Hydraulic Model Investigation. Technical Report HL-87-4. US Army Engineer Waterways Experiment Station.
McDougall, C.A., Blanchfield, P.J., Peake, S.J., Anderson, W.G., 2013. Movement patterns and size-class influence entrainment susceptibility of Lake Sturgeon in a small hydroelectric reservoir. Trans. Am. Fish. Soc. 142, 1508–1521.
McElroy, B., DeLonay, A., Jacobson, R., 2012. Optimum swimming pathways of fish spawning migration in rivers. Ecology 93, 29–34.
Neary, V.S., 2012. Binary fish passage models for uniform and nonuniform flows. River Res. Appl. 28, 418–428.
Nestler, J.M., Goodwin, R.A., Cole, T.M., Degan, D., Dennerline, D., 2002. Simulating movement patterns of blueback herring in a stratified southern impoundment. Trans. Am. Fish. Soc. 131, 55–69.
Noatch, M.R., Suski, C.D., 2012. Non-physical barriers to deter fish movements. Environ. Rev. 20, 71–82.
Otezia, P., Odtricil, I., Lauder, G., Portugues, R., Engert, F., 2017. A novel mechanism for mechanosensory-based rheotaxis in larval zebrafish. Nature 547, 445–448. http://dx.doi.org/10.1038/nature23014.
Peake, S.J., Farrell, A.P., 2006. Fatigue is a behavioural response in respirometer-confined smallmouth bass. J. Fish. Biol. 68, 1742–1755.
Peake, S., Beamish, F.W.H., McKinley, R.S., Scruton, D.A., Katapodis, C., 1997. Relating swimming performance of lake sturgeon, Acipenser fulvescens, to fishway design. Can. J. Fish. Aquat. Sci. 54, 1361–1366.
Pendleton, R.M., Schwinghamer, C., Solomon, L.E., Casper, A.F., 2017. Competition among river planktivores: are native planktivores still fewer and skinner in response to the Silver carp invasion? Environ. Biol. Fish. 100 (10), 1213–1222. http://dx.doi.org/10.1007/s10641-017-0637-7.
Powers, P.D., Bates, K., Burns, T., Gowen, B., Whitney, R., 1997. Culvert Hydraulics Related to Upstream Juvenile Salmon Passage. Washington Department of Fish and Wildlife, Lands and Restoration Services Program, Project 982740. .
Sass, G.G., Hinz, C., Erickson, A.C., McClelland, N.N., McClelland, M.A., Epifanio, J.M., 2014. Invasive bighead and silver carp effects on zooplankton communities in the Illinois River, Illinois, USA. J. Great Lakes Res. 40, 911–921.
Schrank, S.J., Guy, C.S., 2002. Age, growth, and gonadal characteristics of adult bighead carp, Hypophthalmichthys nobilis, in the lower Missouri River. Environ. Biol. Fishes 64, 443–450.
Schrank, S.J., Guy, C.S., Fairchild, J.F., 2003. Competitive interactions between age-0 Bighead Carp and Paddlefish. Trans. Am. Fish. Soc. 132, 1222–1228.
Seibert, J.R., Phelps, Q.E., Yallaly, K.L., Tripp, S., Solomon, L., Stefanavage, T., Herzog, D.P., Taylor, M., 2015. Use of exploitation simulation models for silver carp (Hypophthalmichthys molitrix) populations in several Midwestern US rivers. Manage. Biol. Inv. 6, 295–302.
Spalart, P.R., 2000. Strategies for turbulence modelling and simulations. Int. J. Heat Fluid Flow 21, 252–263.
Staaterman, E., Paris, C.B., 2004. Modelling larval fish navigation: the way forward. ICES J. Mar. Sci. 71, 918–924.
Strand, E., Jørgensen, C., Huse, G., 2005. Modelling buoyancy regulation in fishes with swimbladders: bioenergetics and behaviour. Ecol. Mod. 185, 309–327.
Tripp, S., Brooks, R., Herzog, D., Garvey, J., 2014. Patterns of fish passage in the Upper Mississippi River. River Res. Appl. 30, 1056–1064.
Tsehaye, I., Catalano, M., Sass, G., Glover, D., Roth, B., 2013. Prospects for fishery-induced collapse of invasive Asian carp in the Illinois River. Fisheries 38, 445–454.
Tullos, D., Walter, C., Dunham, J., 2016. Does resolution of flow field observation influence apparent habitat use and energy expenditure in juvenile coho slamon? Water Resour. Res. 52. http://dx.doi.org/10.1002/2015WR018501.
USACE [U.S. Army Corps of Engineers], 2003. Water Control Manual: Mississippi River Nine Foot Channel Navigation Project. Lock and Dam No. 8. Appendix 8 of the Master Water Control Manual. St. Paul District. St. Paul, MN.
USFWS [United States Fish and Wildlife Service], 2014. The First Annual Report to Congress: Summary of Activities and Expenditures to Manage the Threat of Asian Carp in the Upper Mississippi and Ohio River Basins, June 2012 to June 2014. PL 113-121. .
Wilcox, D.B., Stefanik, E.L., Kelner, D.E., Cornish, M.A., Johnson, D.J., Hodgins, I.J., Johnson, B.L., 2004. Improving Fish Passage Through Navigation Dams on the Upper Mississippi River System. USACE. ENV Report 54.
Zielinski, D.P., Sorensen, P.W., 2016. Bubble curtain deflection screen diverts the movement of both Asian and common carp. N. Am. J. Fish. Manage. 36, 267–276.
Zigler, S.J., Dewey, M.R., Knights, B.C., Runstrom, A.L., Steingraeber, M.T., 2003. Movement and habitat use by radio-tagged paddlefish in the upper Mississippi River and tributaries. N. Am. J. Fish. Manage. 23, 189–205.
Zigler, S.J., Dewey, M.R., Knights, B.C., Runstrom, A.L., Steingraeber, M.T., 2004. Hydrologic and hydraulic factors affecting passage of paddlefish through dams in the upper Mississippi River. Trans. Am. Fish. Soc. 133, 160–172.